

Electric field and electric potential due to a finite cylindrical surface charge distribution considering a linearly variable surface charge density

Guillermo A. Díaz^a, Enrique E. Mombello^b and Geovanny A. Marulanda^{a,*}

^a*Universidad de la Salle, Bogota, Colombia*

^b*CONICET – Universidad Nacional de San Juan, San Juan, Argentina*

Abstract. This paper proposes a fast and accurate method for determining the electric potential and the radial and axial components of electric field intensity produced by a finite cylindrical surface charge distribution. The surface charge density has been modeled having a linear variation along the axial dimension of the cylinder. This consideration is very important when large bodies are to be modeled by means of an arrangement of elements (such as finite cylinders, disks, cones, etc.) allowing the matching between them and also avoiding discontinuities on charge distribution. The mathematical expressions presented in this paper have shown high computational performance while ensuring accurate and reliable results.

Keywords: Coulomb's law, electric potential, electric field, semianalytic integral methods

1. Introduction

The calculation of the electric field distribution produced by certain conductor and insulator arrangements is of great importance on the design stage of electrical equipment. The understanding of the spatial distribution of the electric field makes it possible to evaluate the stress on the insulating structures, allowing the detection of critical points that can compromise the safety and lifetime of the device [1].

A large number of methods are available in the literature for solving the electric field produced by complex geometric configurations, such as the Finite Element Method (FEM), the Charge Simulation Method (CSM), the Finite Difference Method (FDM), the Monte Carlo Method (MCM) and the Boundary Element Method (BEM), among others [2].

In addition to the aforementioned methods, there are also semi-analytical calculation techniques. These techniques are commonly based on the solution of elementary geometric configurations such as cylinders, disks, cones, arcs, etc., which by superposition make it possible the modeling of complex geometries with different material properties and boundary conditions.

*Corresponding author: Geovanny A. Marulanda, Universidad de la Salle, Cra 2 # 10-70, 7th floor, Bogota, Colombia. Tel.: +571 3535360 ext.: 2528; E-mail: guandiaz@unisalle.edu.co.

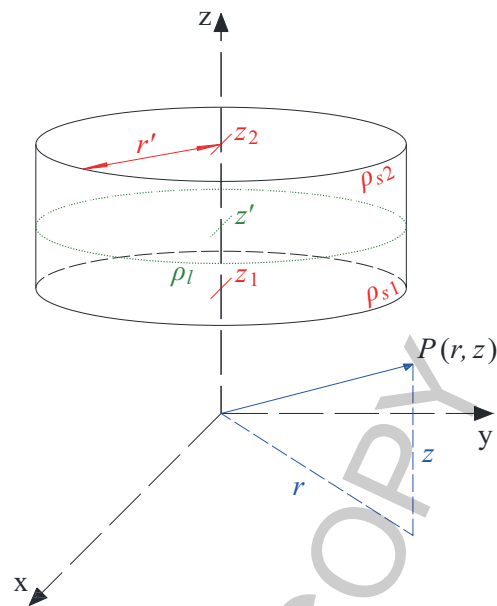


Fig. 1. Cylindrical distribution of surface charge density.

In the article [3], a semi-analytical technique has been successfully applied to predict the nonlinear current distribution in foil windings transformers. In [3] the method has been formulated using the general solutions (for magnetic field) of two different elements, the finite cylinder and the finite disk [4, 5]. Since the solution of these elements is of integral nature, the method was named *Semianalytic Integral Method* (SAIM).

It was found an important improvement on computational performance using SAIM if compared with traditional methods such as FEM, since SAIM only needs to discretize the boundary between two different materials, allowing a significant reduction of the problem size and calculation times [3].

The authors of this work have found a great potential in extending the scope of SAIM proposed in [3] to electric field problems. The aim of this paper is to provide the mathematical expressions for determining the electric potential and electric field of one of the basic elements of SAIM, which is the cylindrical sheet of charge with linear surface charge distribution.

The expressions presented in this article can be also used to approximate the electric field produced by generic cylindrical configurations which appear quite frequently in practical engineering applications. According to the knowledge of the authors of this work, field expressions for a thin cylindrical charge distribution considering linear variation of the surface charge has not been yet presented in the literature; in fact, no publications have been found considering constant charge density either.

1.1. Statement of the problem

The aim of this paper is to propose efficient mathematical expressions for determining the electric potential V and the components of the electric field intensity in radial direction E_r and axial direction E_z produced by a finite cylindrical surface charge distribution at an arbitrary observation point $P(r, z)$.

The geometry of the problem to be solved is presented in Fig. 1, where the charge distribution is considered to have a value of ρ_{s1} (C/m^2) at the bottom of the cylinder, and varies linearly up to the top,

where the charge density is ρ_{s2} (C/m²). The coordinates of the base and the top of the cylindrical charge distribution are denoted by z_1 (m) and z_2 (m) respectively, while its radius is denoted by the variable r' (m).

A filamentary loop with uniform line charge density ρ_l (C/m) has also been considered, having its center on the z axis at z' , where $z_1 \leq z' \leq z_2$. Notice that the radius of the loop is also r' .

1.2. Basic mathematical expressions

The starting point for solving the problem is the mathematical expression of the electric potential produced by the filamentary loop with charge density ρ_l . By applying Coulomb's law for distributed charges [6], the following expression is obtained for the electric potential at an arbitrary observation point $P(r, z)$.

$$V^{[fl]} = \frac{1}{4\pi\epsilon_0} \int_0^{2\pi} \frac{\rho_l r' d\phi'}{\sqrt{r^2 + r'^2 + (z - z')^2 - 2rr' \cos(\phi')}} \quad (1)$$

where ϵ_0 is the electric permittivity of vacuum and ϕ' is the azimuthal angle. Notice that primed coordinates have been used to indicate their association with the field source, while not primed coordinates are associated with the observation point. On the other hand, the superscript in electric potential $[fl]$ makes reference to *filamentary loop*. The surface charge density of the cylinder is linearly distributed from its base (z_1) to its top (z_2), which can be written mathematically by means of the following relationship

$$\rho_s(z') = \frac{\rho_{s2} - \rho_{s1}}{z_2 - z_1}(z' - z_1) + \rho_{s1} \quad (2)$$

According to the above, the line charge density associated with a circular segment of a circular cylinder of differential height dz' is

$$\rho_l = \rho_s(z') dz' \quad (3)$$

Substituting Eq. (3) in Eq. (1) and integrating from z_1 to z_2 , the expression for the electric potential produced by a cylindrical charge distribution is obtained

$$V = \frac{1}{4\pi\epsilon_0} \int_{z_1}^{z_2} \int_0^{2\pi} \frac{\rho_s(z') r'}{\sqrt{r^2 + r'^2 + (z - z')^2 - 2rr' \cos(\phi')}} d\phi' dz' \quad (4)$$

Notice that the superscript $[fl]$ has been removed because from this point all the expressions will refer to the cylindrical distribution of charge. It is convenient to define the function

$$f_V(\phi', z') = \frac{\rho_s(z') r'}{\sqrt{r^2 + r'^2 + (z - z')^2 - 2rr' \cos(\phi')}} \quad (5)$$

which will be useful in developing the following formulations. Thus, the electric potential can be expressed in a simpler way as follows

$$V = \frac{1}{4\pi\epsilon_0} \int_{z_1}^{z_2} \int_0^{2\pi} f_V(\phi', z') d\phi' dz' \quad (6)$$

Since $f_V(\phi', z')$ is an even function with respect to ϕ' , it is possible to rewrite its expression as follows

$$V = \frac{2}{4\pi\epsilon_0} \int_0^\pi \int_{z_1}^{z_2} f_V(\phi', z') dz' d\phi' \quad (7)$$

Additionally, note that the order of integration has been intentionally reversed. Since for static electric fields the curl is zero $\nabla \times \vec{E} = \vec{0}$, the electric field can be expressed as the gradient of a scalar field as follows,

$$\vec{E} = -\nabla V \quad (8)$$

where the minus sign in Eq. (8) is associated with physical considerations of potential energy. The gradient of the electric potential in cylindrical coordinates is

$$\nabla V = \hat{r} \frac{\partial V}{\partial r} + \hat{\phi} \frac{1}{r} \frac{\partial V}{\partial \phi} + \hat{z} \frac{\partial V}{\partial z} \quad (9)$$

Because the surface charge density is constant in the direction of the azimuthal angle, there are no changes in the electric potential in this direction, so that $\partial V / \partial \phi = 0$. Substituting the corresponding components of the electric field strength into Eq. (9), it becomes,

$$\vec{E} = \hat{r} E_r + \hat{z} E_z = -\hat{r} \frac{\partial V}{\partial r} - \hat{z} \frac{\partial V}{\partial z} \quad (10)$$

Substituting Eqs (7) into (10) the radial and axial components of the electric field can be identified. Accordingly, the radial component is,

$$E_r = -\frac{2}{4\pi\epsilon_0} \int_0^\pi \int_{z_1}^{z_2} \frac{\partial}{\partial r} (f_V(\phi', z')) dz' d\phi' \quad (11)$$

and the axial component is,

$$E_z = -\frac{2}{4\pi\epsilon_0} \int_0^\pi \int_{z_1}^{z_2} \frac{\partial}{\partial z} (f_V(\phi', z')) dz' d\phi' \quad (12)$$

2. Solution methodology

The next step is to find the solutions of Eqs (7), (11) and (12). In some engineering problems the value of the surface charge densities ρ_{s1} and ρ_{s2} are known, so that the task is simply to determine the value of the potential or the electric field intensity at some point in space. However, in many applications only some boundary conditions are known and the problem consists in determining the value of the charge densities that satisfy the boundary conditions imposed. For the above reason, it is important to find mathematical expressions which consider separately the geometry from the effect due to charge densities. According to the above, it can be shown that the electric potential can be written as,

$$V = k_{V1}\rho_{s1} + k_{V2}\rho_{s2} \quad (13)$$

where k_{V1} and k_{V2} are real numbers which depend only on the geometry of the field source and on the coordinates of the observation point, so that they are referred to as *geometry dependent factors*. Similarly, the following equations for the radial and axial components of the electric field can be written,

$$E_r = k_{r1}\rho_{s1} + k_{r2}\rho_{s2} \quad (14)$$

$$E_z = k_{z1}\rho_{s1} + k_{z2}\rho_{s2} \quad (15)$$

Consequently, the overall objective of this work is to determine the mathematical expressions for geometry dependent factors k_{V1} , k_{V2} , k_{r1} , k_{r2} , k_{z1} y k_{z2} .

3. Analytical integrals with respect to z'

The analytical solution of the integral Eqs (7), (11) and (12) with respect to z' are presented in this section. As already seen in Section 2, the solution of the integrals is based on the determination of the geometry dependent factors. The expressions presented in this section are quite compact and include basic functions like cosine and logarithm, which ensures a fast numerical calculation.

3.1. Electric potential

According to Eqs (7) and (13), the electrical potential is,

$$V = \frac{2}{4\pi\epsilon_0} \int_0^\pi \int_{z_1}^{z_2} f_V(\phi', z') dz' d\phi' = k_{V1}\rho_{s1} + k_{V2}\rho_{s2} \quad (16)$$

The geometry dependent factors can be expressed as,

$$k_{V1} = \frac{2}{4\pi\epsilon_0} \int_0^\pi \left(s_V \Big|_{z_i=z_2} \Big|_{z'=z_1}^{z'=z_2} \right) d\phi' \quad (17)$$

$$k_{V2} = -\frac{2}{4\pi\epsilon_0} \int_0^\pi \left(s_V \Big|_{z_i=z_1} \Big|_{z'=z_1}^{z'=z_2} \right) d\phi' \quad (18)$$

where

$$s_V = \frac{1}{z_1 - z_2} r' (\xi_4 + (z_i - z) \ln(z - z' + \xi_4)) \quad (19)$$

$$\xi_1 = (z - z')^2 \quad (20)$$

$$\xi_2 = r^2 + r'^2 - 2rr' \cos(\phi') \quad (21)$$

$$\xi_3 = \xi_1 + \xi_2 \quad (22)$$

$$\xi_4 = \sqrt{\xi_3} \quad (23)$$

Notice that intermediate variables such as $\xi_1 \dots \xi_4$ have been intentionally introduced. In electric field problems the values of the three quantities (V , E_r and E_z) are normally required, so the intermediate variables allow improving the computational performance through the reuse of calculations.

The electric potential V will demand a higher initial computational effort, however the calculation of E_r and E_z result almost trivial since the expressions for these last two quantities are rather simple because they rely on the intermediate variables.

The reader may wonder whether it is worth introducing intermediate variables, therefore it is important to highlight that the computational savings are much more evident and profitable when there are hundreds or thousands of field sources and observation points, which is a normal situation when modeling complex electrical equipment such as transformers, generators, etc.

3.2. Field strength in the radial direction

According to Eqs (11) and (14), the electric field intensity in the radial direction is,

$$E_r = -\frac{2}{4\pi\epsilon_0} \int_0^\pi \int_{z_1}^{z_2} \frac{\partial}{\partial r} (f_V(\phi', z')) dz' d\phi' = k_{r1}\rho_{s1} + k_{r2}\rho_{s2} \quad (24)$$

The geometry dependent factors can be expressed as,

$$k_{r1} = -\frac{2}{4\pi\epsilon_0} \int_0^\pi \left(s_r \Big|_{z_i=z_2} \Big|_{z'=z_1}^{z'=z_2} \right) d\phi' \quad (25)$$

$$k_{r2} = \frac{2}{4\pi\epsilon_0} \int_0^\pi \left(s_r \Big|_{z_i=z_1} \Big|_{z'=z_1}^{z'=z_2} \right) d\phi' \quad (26)$$

where

$$s_r = \frac{r'(r - r' \cos(\phi')) (\xi_2 + (z - z_i)(z - z'))}{(z_1 - z_2) \xi_2 \xi_4} \quad (27)$$

3.3. Field strength in the axial direction

According to Eqs (12) and (15), the electric field intensity in the axial direction is,

$$E_z = -\frac{2}{4\pi\epsilon_0} \int_0^\pi \int_{z_1}^{z_2} \frac{\partial}{\partial z} (f_V(\phi', z')) dz' d\phi' = k_{z1}\rho_{s1} + k_{z2}\rho_{s2} \quad (28)$$

The geometry dependent factors can be expressed as,

$$k_{z1} = -\frac{2}{4\pi\epsilon_0} \int_0^\pi \left(s_z \Big|_{z_i=z_2} \Big|_{z'=z_1}^{z'=z_2} \right) d\phi' \quad (29)$$

$$k_{z2} = \frac{2}{4\pi\epsilon_0} \int_0^\pi \left(s_z \Big|_{z_i=z_1} \Big|_{z'=z_1}^{z'=z_2} \right) d\phi' \quad (30)$$

where

$$s_z = -\frac{r'}{z_1 - z_2} \left(\frac{z' - z_i}{\xi_4} - \ln(z' - z + \xi_4) \right) \quad (31)$$

As shown in Eqs (17), (18), (25), (26), (29) and (30), the new variable z_i has been introduced. This new variable allows the calculation of the two geometry dependent factors from one generic expression. For example, in the case of electric potential, the two geometry dependent factors k_{V1} and k_{V2} arise when evaluating s_V with $z_i = z_2$ and $z_i = z_1$ respectively.

4. Integrals with respect to ϕ'

As presented above, the mathematical expressions for the integrals with respect to z' are now available. In order to find the geometry dependent factors, it is necessary to evaluate the integrals Eqs (17), (18), (25), (26), (29) and (30) with respect to ϕ' . Unfortunately, it has been found that these integrals do not have a closed analytical solution so that it is necessary to evaluate them numerically. For this purpose, using a matrix based integration method (such as the one the introduced in [5]) is strongly recommended when there are a large quantity of sources and evaluation points.

It is worth mentioning that if the decision to solve the integrals by means a quadrature is taken, it is recommended to use an *open type* strategy for node allocation [7]. This is because the expressions for s_V , s_r and s_z produce a singularity when $z = z'$, $r = r'$ and $\phi' = 0$. Accordingly, if a *closed type* node allocation strategy is used and the evaluation point is at one end of the cylinder, the integration routine will inevitably leads to an indetermination [7].

Although it has been found that the mathematical expressions for the electric potential and the radial electric field do not have a closed analytical solution, it has been found that it is actually possible to obtain expressions for the axial component of the electric field as function of complete elliptic integrals as presented below.

$$\int_0^\pi s_z d\phi' = \frac{r'(\zeta_1 + \zeta_2 + \zeta_3)}{r(r+r')(z_1 - z_2)\sqrt{(r+r')^2 + (z-z')^2}} \quad (32)$$

with the intermediate variables,

$$\zeta_1 = E(\eta)(r+r')\left((r+r')^2 + (z-z')^2\right) \quad (33)$$

$$\zeta_2 = K(\eta)(r+r')(r^2 - r'^2 + (z-z')(z' - z_i)) \quad (34)$$

$$\zeta_3 = \Pi(\alpha^2, \eta)(r-r')(z-z_i)(z-z') \quad (35)$$

$$\eta = \frac{4rr'}{r^2 + 2rr' + r'^2 + (z-z')^2} \quad (36)$$

$$\alpha^2 = \frac{4rr'}{(r+r')^2} \quad (37)$$

where the functions K , E and Π are complete elliptic integrals of the first, second and third kind respectively [8,9]. In the case of the equations related to the electric potential and the radial component of electric field (s_V and s_r), expressions such as

$$\log\left(z' - z + \sqrt{r^2 + r'^2 + (z-z')^2 - 2rr' \cos(\phi')}\right) \quad (38)$$

appear, for which the integrals respect to ϕ' unfortunately cannot be written in terms of complete elliptic integrals [6]. It is worth mentioning that in reference [4], where the mathematical expressions for the magnetic field of the finite cylinder were presented, all the integrals obtained can be expressed in terms of complete elliptic integrals.

5. Results and validation

The validity of the expressions presented in this paper has been verified by calculating several hundred of random cases which were compared with the results obtained using the routine `integral2`

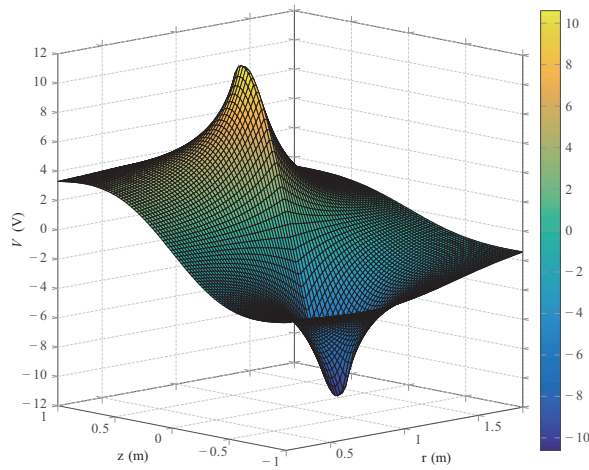


Fig. 2. Electric potential due to the charge distribution.

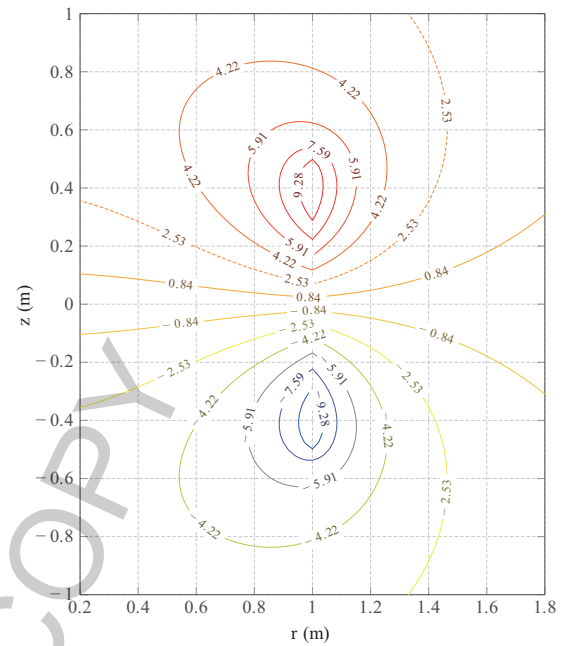


Fig. 3. Equipotential lines due to the charge distribution (values in volts).

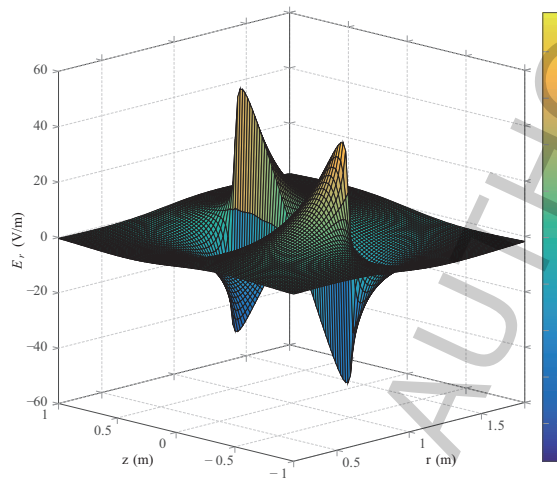


Fig. 4. Radial component of the electric field due to the charge distribution.

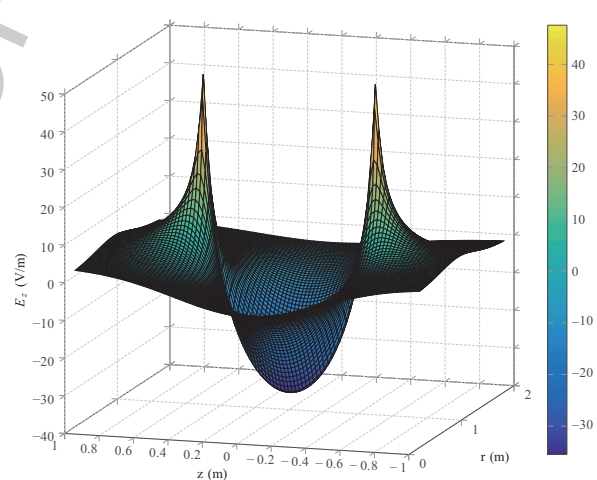


Fig. 5. Axial component of the electric field due to the charge distribution.

of Matlab. Satisfactory results were found for all analyzed cases. In order to illustrate the performance of the calculation method, the results of a specific case is presented, which makes it possible to visualize the field distribution produced by the cylindrical charge sheet and also to give an insight into the computational performance of the proposed expressions. The dimensions of the case study are $r' = 1$ m, $z_1 = -0.5$ m, $z_2 = 0.5$ m with surface charge densities $\rho_{s1} = -1$ nC/m² and $\rho_{s2} = 1$ nC/m². The electric potential and the electric field in radial and axial directions have been evaluated on a regular grid

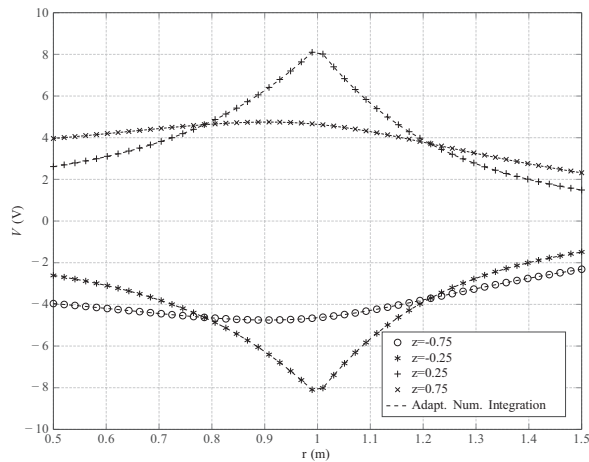


Fig. 6. 2D plot of the electrical potential due to the cylindrical charge sheet.

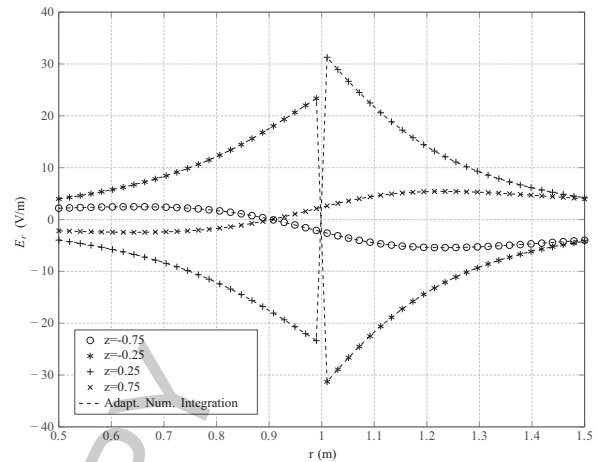


Fig. 7. 2D plot of the radial component of the electric field due to the cylindrical charge sheet.

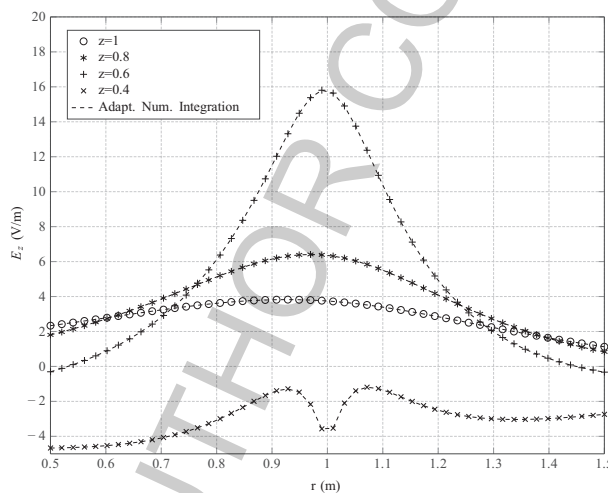


Fig. 8. 2D plot of the axial component of the electric field due to the cylindrical charge sheet.

of $100 \times 100 = 10000$ points. The average time spent by Matlab to calculate V , E_r and E_z at every point of the grid using the proposed formulation with the matrix based integration method was 0.72 seconds. Furthermore, the evaluation just for the electric potential on the same grid using the numerical integration routine `integral2` takes on average 60.3 seconds. If the radial and axial components are included into the numerical integration using `integral2` the total average time is close to 4 minutes. The calculations were performed on a computer with a processor Core i7 2.00 GHz and 16 GB RAM. Figs 2 to 5 show the results of the case study. It can be seen in Fig. 2 that the electric potential is positive on the upper half of the cylinder, while it is negative on the bottom half, which is due to the change of sign of the surface charge density in the central part of the cylinder. Figure 3 shows the distribution of equipotential lines, in which it is clearly evident that the potential inside and outside the cylinder is not symmetric as a result of the rotational symmetry of the problem.

Figure 4 shows the electric field distribution in the radial direction. As it can be seen, a discontinuity

arises in the radial component on either side of the cylinder. Figure 5 shows the distribution of the axial electric field, which undergoes a dramatic increase near the ends of the cylinder.

An excellent agreement has been found by comparing the results calculated using the formulas proposed in this work and the ones obtained by double adaptive numerical integration of the original Eqs (7), (11) and (12). A comparison between the results obtained using the proposed formulation and the ones using adaptive numerical integration is presented in Figs 6, 7 and 8.

6. Conclusions

This paper presents mathematical expressions to determine the electric potential and the electric field produced by a cylindrical surface charge distribution considering a linear variation of the surface charge density in the axial direction.

It was found that the proposed methodology is considerably faster than traditional calculations performed by means of the double adaptive numerical integration preserving an adequate precision for engineering purposes.

It is important to note that the problem of considering a constant cylindrical charge distribution is a particular case of the problem presented in this paper, which can be easily considered simply by assigning $\rho_{s1} = \rho_{s2} = \rho_{sc}$, where ρ_{sc} would correspond to the constant surface charge of the cylinder.

Even though it was found that the expressions for V and E_r cannot be expressed in terms of complete elliptic integrals, the closed analytic expression for the axial component of electric field E_z was presented.

Acknowledgments

This work has been supported by La Universidad de la Salle Bogota and the CONICET – Universidad Nacional de San Juan Argentina. The authors acknowledge for the interest and continuous support to this project.

References

- [1] R. Maheswari, P. Subburaj, B. Vigneshwaran and L. Kalaivani, Non linear support vector machine based partial discharge patterns recognition using fractal features, *Journal of Intelligent & Fuzzy Systems: Applications in Engineering and Technology* **27**(5) (2014), 2649–2664.
- [2] Z.P. Bai, Numerical analysis of electromagnetic fields, Springer, 1993.
- [3] G. Díaz and E. Mombello, Semianalytic integral method for fast solution of current distribution in foil winding transformers, *Magnetics, IEEE Transactions on* **51** (Sept 2015), 1–9.
- [4] G. Díaz, E. Mombello and V. Stephan, Magnetic vector potential and magnetic field intensity due to a finite current carrying cylinder considering a variable current density along its axial dimension, *International Journal of Applied Electromagnetics and Mechanics* **40**(2) (2012), 133–147.
- [5] G. Díaz and E. Mombello, Magnetic field due to a finite current carrying disk considering a variable current density along its radial dimension, *International Journal of Applied Electromagnetics and Mechanics* **42**(1) (2013), 119–136.
- [6] P. Solin, I. Dolezel, P. Karban and B. Ulrych, Integral methods in low-frequency electromagnetics, John Wiley & Sons, 2009.
- [7] P.K. Kythe and M.R. Schäferkötter, Handbook of computational methods for integration. CRC Press, 2004.
- [8] D. Lozier, R. Boisvert and C. Clark, Nist handbook of mathematical functions, Cambridge University Press, 2010.
- [9] I.A. Stegun and M. Abramowitz, Handbook of Mathematical Functions, with Formulas, Graphs, and Mathematical Tables. Dover Publications, 1964.